C. Schott, W. Zinn, B. Scholtes, T. Niendorf

Bend Straightening of a Carbonitrided Gear Shaft – Consequences on Residual Stresses and Retained Austenite near the Surface*

Biegerichten einer carbonitrierten Getriebewelle – Auswirkungen auf randnahe Eigenspannungen und Restaustenitgehalte

Abstract/Kurzfassung

Carbonitriding of shafts in drive technology is strongly connected with distortion. Bend straightening is an important process step in order to eliminate distortion without removing the hardened surface layer. As shown in several investigations, even for simple part geometries, bending induced stresses and plastic deformations have a strong impact not only on the residual stress state but also on the microstructure after straightening. As gear shafts become increasingly filigree and complex in their geometry, the components state after straightening is only understood in rare cases. Due to indispensable, function based notches as well as changes in the cross section, these effects will occur especially in areas of small cross sections or notches in conjunction with high bending stresses. It is the objective of this work, to characterize these critical areas with respect to the distribution of residual stresses and retained austenite along the circumference as well as in the in-depth direction. Therefore, the measured distributions of residual stresses, integral width values and retained austenite near the surface will be presented and discussed. For this purpose a carbonitrided gear shaft taken out of a large production volume was investigated before and after a commonly used straightening operation. ■

Keywords: Bend straightening, carbonitriding, residual stresses, retained austenite, drive shaft

In der Antriebstechnik stellt das Biegerichten nach der Einsatzhärtung von Wellen einen wichtigen Prozessschritt dar, um den oftmals unvermeidlichen Verzug zu beseitigen und gleichzeitig die harte Randschicht des Bauteils zu erhalten. Wie bereits in einigen Untersuchungen dargestellt wurde, beeinflussen die beim Richten vorliegenden Spannungen und die daraus resultierenden plastischen Deformationen sowohl den Eigenspannungszustand als auch die Mikrostruktur schon bei geometrisch simplen Bauteilen. Für die zunehmend filigranen und in ihrer Geometrie komplexen Wellen ist der Zustand nach dem Richten jedoch nur in seltenen Fällen bekannt und nachvollziehbar. Bei einer Welle, die konstruktiv notwendige Querschnittsänderungen oder auch Kerben aufweist, werden die genannten Effekte dort auftreten, wo Bereiche mit geringem Querschnitt und solche mit hohen Lastspannungen durch den Richtprozess zusammenfallen. Ziel dieser Arbeit ist es, diese kritischen Bereiche im Hinblick auf die Verteilung von Eigenspannungen und Restaustenit, sowohl entlang des Umfangs als auch in Tiefenrichtung, detailliert zu charakterisieren, um ein besseres Verständnis für den Zustand gerichteter Wellen zu gewinnen. Dazu werden die ermittelten randnahen Eigenspannungsverläufe und die Verteilungen der Integralbreiten sowie der Restaustenitgehalte am Beispiel einer in großer Stückzahl hergestellten Getriebewelle vor und nach einem praxisüblichen Richtprozess vorgestellt und diskutiert. ■

Schlüsselwörter: Biegerichten, Carbonitrieren, Eigenspannungen, Restaustenit, Antriebswelle

Autoren/Authors: ***Dipl.-Ing Christopher Schott,*** Institut für Werkstofftechnik – Metallische Werkstoffe, Universität Kassel, Mönchebergstraße 3, 34125 Kassel, c.schott@uni-kassel.de (Kontakt/Corresponding author)
Dr.-Ing. Wolfgang Zinn, Prof. Dr.-Ing. habil. Berthold Scholtes, Prof. Dr.-Ing. Thomas Niendorf, Institut für Werkstofftechnik – Metallische Werkstoffe, Universität Kassel

* Lecture at the HK 2016, 72nd HeatTreatmentCongress, 26-28 October 2016 in Cologne, Germany

1 Introduction

In order to achieve the requirements for drive shafts in terms of fatigue strength, they are usually carburized or carbonitrided [1]. Massive efforts are made to avoid heat treatment dependend distortion as it causes enormous costs [2, 3]. Like it is shown in many investigations, the carriers for distortion potential cannot be found solely in the heat treatment process itself, but in the complete production history [4]. In most cases distortion has to be corrected by straightening, since grinding would remove parts of the hardened surface layer. Unavoidable consequences of the straightening process are cracked shafts and elongation of the cycle time [5]. Even if the shaft is straightened successfully, the impact of the straightening operation on the microstructure and the residual stress state is not sufficiently known. The typical residual stress state after case hardening, which improves the fatigue properties, is characterized by compressive residual stresses below the surface. Locally limited plastic deformations, that are responsible for the straightening work, change this residual stress state significantly [6, 7]. Furthermore, the defined amount of retained austenite that was adjusted during heat treatment will transform partly to martensite which causes microstructural inhomogeneity around the circumference. [8]. The effects of bend straightening on the materials properties were investigated in many different works, whereby sample geometry and degree of straightening differ from realistic conditions [9–13]. Typically bending tests are carried out on even samples for the purpose of geometry-independent statements. Furthermore higher degrees of bending are chosen to maximize the expected effects. However real drive shafts show design- and function-based notches that will create stress concentrations in the notched areas. Thus plastic deformations will be locally restricted. Finally, realistic radial runout deviations are comparatively smaller so that equally small plastic deformations are required for the straightening work. As a consequence the focus is on the area that plastifies first. These areas are characterized by high stresses that meet low yield points. During the bending process, load induced stresses superimpose with initial residual stresses and the highest stresses are to be expected where stresses of the same sign meet. As carburized or carbonitrided parts usually show surface damage the yield point is lowest directly on the surface [14]. Hereafter these assumptions are investigated on a hollow shaft that is used in an automobile gearbox. For this purpose residual stress states and microstructural properties before and after straightening are measured by X-ray diffraction and compared around the circumference as well as in depth direction.

C	Si	Mn	P	S	Cr	Mo	Ni	Al
0.15-0.23	≤ 0.12	0.5-0.8	≤ 0.035	0.025-0.035	0.65-0.85	0.28-0.38	1.5-1.9	0.015-0.040

Fig. 1. The investigated drive shaft and the steel composition in mass-%

Bild 1. Die untersuchte Getriebewelle und die Stahlzusammensetzung in Masse-%

2 Testing material and conditions

The object of investigation is a hollow shaft made out of the material 20NiMoCr6-5 which is used in an automobile gearbox (see Figure 1). The overall length of the shaft is about 249 mm and the outer diameter on the pinion is about 72 mm. Before carbonitriding the microstructure was ferritic-pearlitic. The shaft was carbonitrided in a pusher type furnace (see Table 1 for conditions) and

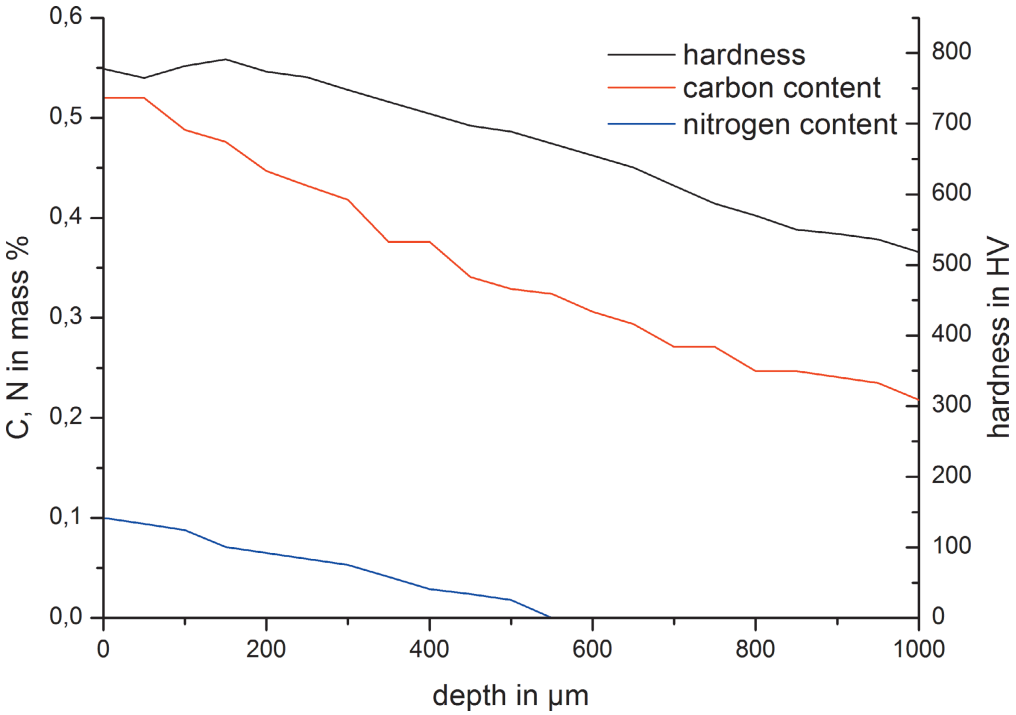

Fig. 2. Depth distributions of hardness as well as C- and N-content

Bild 2. Randnahe Tiefenverteilung der Härte sowie des C- und N-Gehalts

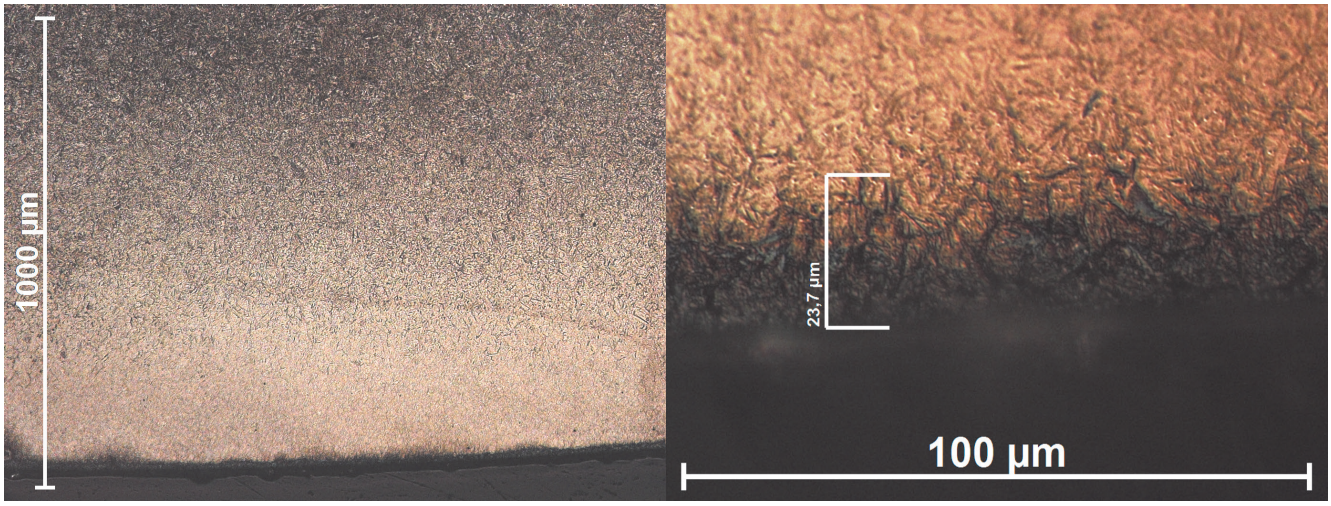

Fig. 3. Martensitic microstructure of the surface area, magnification 100× (left) and 1000× (right)

Bild 3. Martensitisches Gefüge in der Randschicht, Vergrößerung 100× (links) und 1000× (rechts)

quenched in oil (60 °C). Endogas was used to prevent oxidation and the carbon content was set with propane, in addition ammonia gas provided nitrogen. As it is shown in Figure 2, the carbon content on the surface is about 0.52 mass% and the case hardening depth is about 0.9 mm. The nitrogen content immediately at the surface is about 0.1 mass%. The hardness values show a typical distribution including a maximum 0.17 mm below the surface and remain at about 780 HV directly on the surface. After carbonitriding the shaft shows a martensitic microstructure with plate martensite on the surface and lath martensite in the core like it is illustrated in Figure 3. Furthermore a damaged surface layer of about 24 µm can be detected. The straightening operation took place before tempering and was carried out by an automatic straighten-

Zone	1	2	3	4
Time in min	65	65	65	65
Temperature in °C	950	999	980	910
Endogas in m³/h	11	11	16	
Ammonia gas in m³/h	0.6	0.3	–	

Table 1. Carbonitriding paramter

Tabelle 1. Parameter des Carbonitrierprozesses

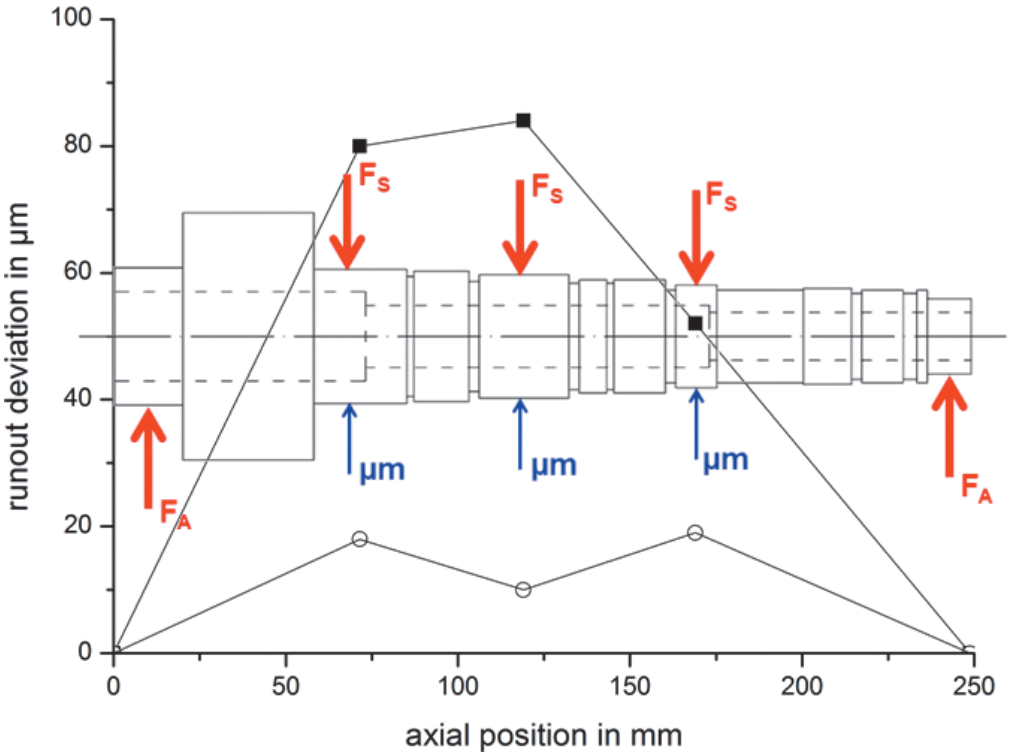

Fig. 4. Axial positions of the measuring and straightening points as well as results of the radial runout deviation measurements before and after straightening

Bild 4. Axiale Positionen der Mess- und Richtstellen sowie Rundlaufabweichungen vor und nach dem Richtprozess

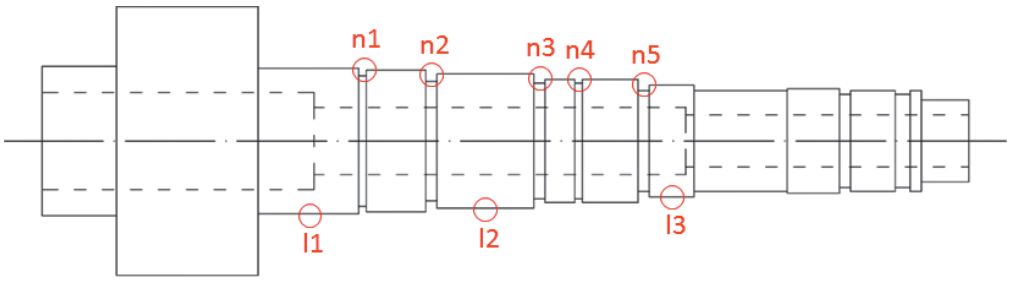

Fig. 5. Axial positions of the different measuring circumferences

Bild 5. Axiale Positionen der jeweiligen Messungen über den Umfang

ing machine (type MAE). The straightening operation starts by positioning the shaft between two center points. Then the shaft is rotated in order to measure the radial runout deviation on three different locations. The results are shown in Figure 4. In this case the radial runout deviation was between 52 µm and 84 µm (blue arrows). In the next step the shaft is supported by two anvils at both ends and gets straightened by a stamp at the same positions that were measured before. The straightening force is applied step by step and increases each time. After the straightening operation the radial runout deviations remained between 10 µm and 19 µm and fulfilled the requirements. It is obvious that the main straightening work was done in the middle position. In order to identify the effects of straightening on the stress state and the microstructure, longitudinal residual stresses, integral widths and the amount

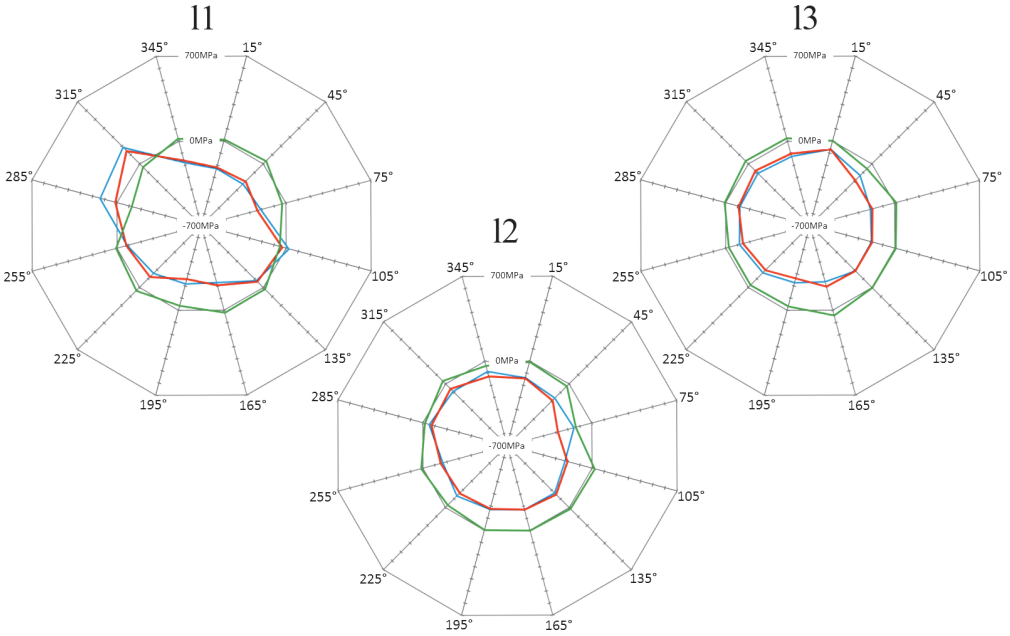

Fig. 6. Longitudinal residual stresses along the circumference on the cylindrical sections before straightening (blue) after straightening (red) and compared to each other (green)

Bild 6. Längseigenspannungen entlang des Umfangs auf der Mantelfläche vor dem Richten (blau), nach dem Richten (rot) sowie deren Differenz (grün)

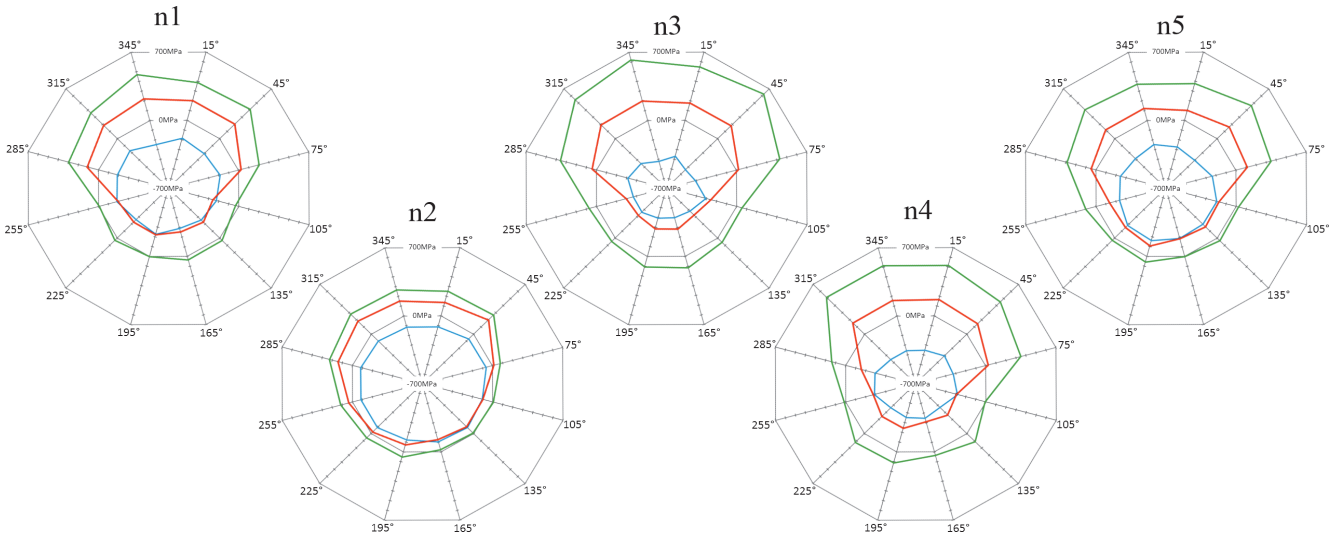

Fig. 7. Longitudinal residual stresses along the circumference on the notches before straightening (blue) after straightening (red) and compared to each other (green)

Bild 7. Längseigenspannungen entlang des Umfangs in den Kerben vor dem Richten (blau), nach dem Richten (rot) sowie deren Differenz (grün)

of retained austenite were measured using X-ray diffraction before and after the straightening process. Altogether about 400 measurements were carried out on a ψ-diffractometer with CrKα radiation. Residual stresses and integral widths were determined using the standard $\sin^2\psi$ method [15] on the {211}-planes, considering 11 angles between −45° and 45°. For measurements on the cylindrical sections a ∅2 mm collimator was used and due to the geometrical restrictions, the diameter had to be reduced to ∅1 mm while measuring in the notches. Diffraction elastic constants $s_1 = -1.33E^{-6}$ MPa^{-1} and ½ $s_2 = 6.095E^{-6}$ MPa^{-1} were used to calculate stresses from the measured lattice strain distributions. The amount of retained austenite was measured on the same diffractometer but only using the Ω-mode. Here the α-Fe planes {211} and {200} as well as the γ-Fe planes {220} and {200} were compared. Since X-ray diffraction gains information directly from the surface, material had to be removed in order to obtain gradients in depth direction, therefore material was step by step removed. Although the removal of material has an influence on the residual stress state, no layer removal correction was done.

3 Surface measurements

In order to compare the residual stress states and integral width values of the shaft before and after the straightening operation, measurements were at first only possible directly on the surface. Therefore measurements were done on eight different axial locations. Three of them are located on the cylindrical sections at the

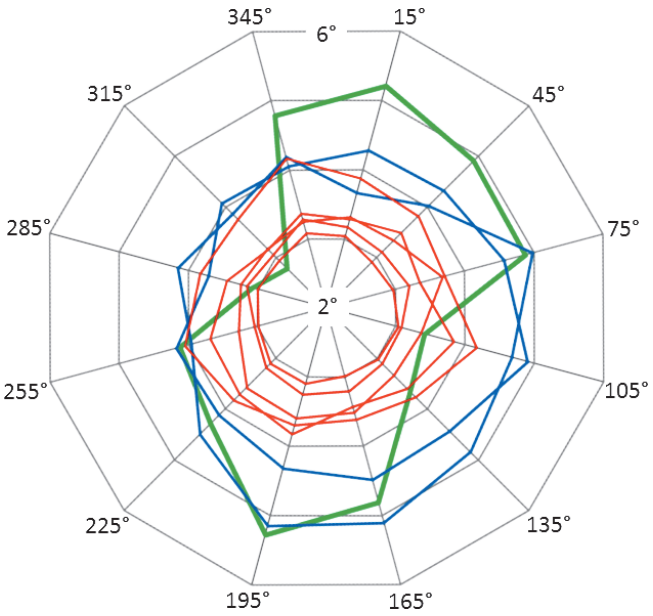

Fig. 8. Integral width values along the circumference on the lateral surface (location l1 green, location l2 and l3 blue) and the notches (red)

Bild 8. Integralbreiten entlang des Umfangs auf der Mantelfläche (Messstelle l1 grün, Messstellen l2 und l3 blau) und in den Kerben (rot)

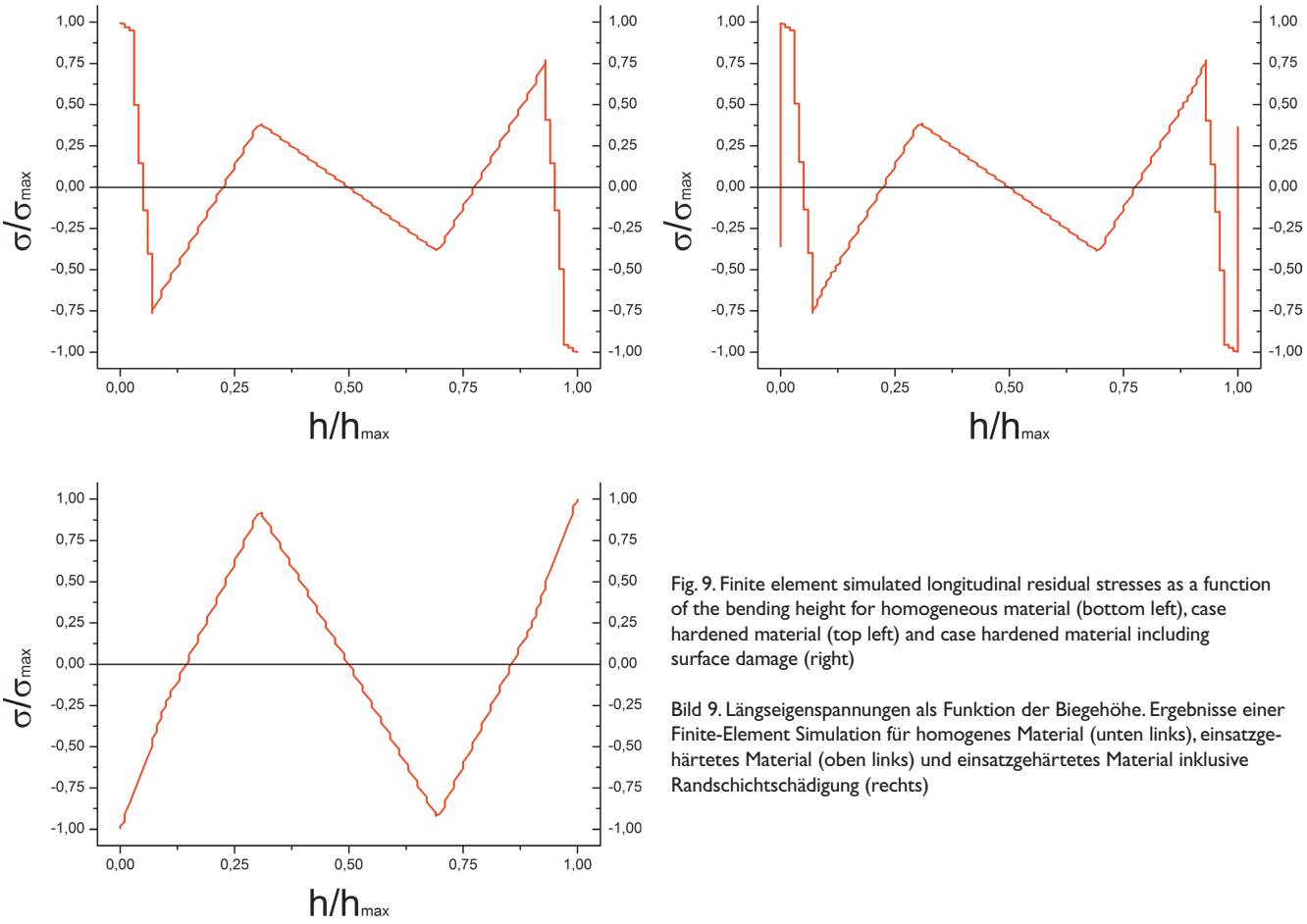

Fig. 9. Finite element simulated longitudinal residual stresses as a function of the bending height for homogeneous material (bottom left), case hardened material (top left) and case hardened material including surface damage (right)

Bild 9. Längseigenspannungen als Funktion der Biegehöhe. Ergebnisse einer Finite-Element Simulation für homogenes Material (unten links), einsatzgehärtetes Material (oben links) und einsatzgehärtetes Material inklusive Randschichtschädigung (rechts)

radial runout deviation measuring points of the straightening process. The other five are located in the different notches in the straightening area. As it is shown in Figure 5 the measuring locations are numbered. Each individual circumference was divided into 30° sections so that 12 measurements describe the stress state at every axial location. The results of the cylindrical sections are shown in Figure 6. In order to relate the stress state to the straightening direction the stress values are shown in polar plots, in which the stamp position is at 0°. The initial residual stress values after carbonitriding are shown in blue, after straightening in red and the difference between those two is shown in green. At first it can be seen, that after carbonitriding the initial residual stress values are about −200 MPa. After straightening the residual stress state hasn't changed at all. The only conspicuous values are situated on measuring location l1 on the 315° and 105° positions. Here even tensile residual stresses exist in the initial state. Possible reasons for that could be different quenching conditions due to the proximity of the high mass pinion or different conditions during carbonitriding because the holding fixture during the heat treatment was placed around measuring location l1. Looking at the notches (see Figure 7) the results differ completely. The initial residual stress values reach from −100 MPa in notch n2 to −500 MPa in notch n3. Different diffusion and quenching conditions that depend on the exact geometry of each notch could be the reason for that. After straightening the stress state on the surface has clearly changed. Looking at the green curves, that describe the difference of residual stresses before and after straightening, it can be seen, that the changes are limited to the compression loaded area. Residual stresses are formed due to plastic deformations which appear during the straightening operation. Plastic deformation takes place where local stresses pass the elastic range. In this case, as the straightening force increases, initial compressive residual stresses from the carbonitriding process superimpose with load stresses. This effect can be seen between the −45° and the 45° positions. On the tension loaded side, compressive residual stresses superimpose with tensile load stresses and the yield stress is not reached. As a result of the straightening process, tensile residual stresses of about 200 MPa are located in each of the notches on the compression loaded side whereas the residual stresses on the tensile loaded side remain unchanged. Hence an asymmetric residual stress state over the shaft circumference has formed. This is particular remarkable because the notch areas will be the most stressed areas of the shaft in use. The integral width values of the different measuring circumferences are displayed in Figure 8. Values from the notched areas are shown in red, those from the cylindrical sections are displayed in blue (measuring location l2 and l3) and green (measuring location l1). It can be seen that the integral width values of the notched areas are systematically lower than those from the lateral surface. Reasons for that could be the same as mentioned above. Furthermore the green curve, which describes measuring location l1 shows lower values at the 315° and 105° position. This matches the positions of tensile residual stresses as seen in Figure 6.

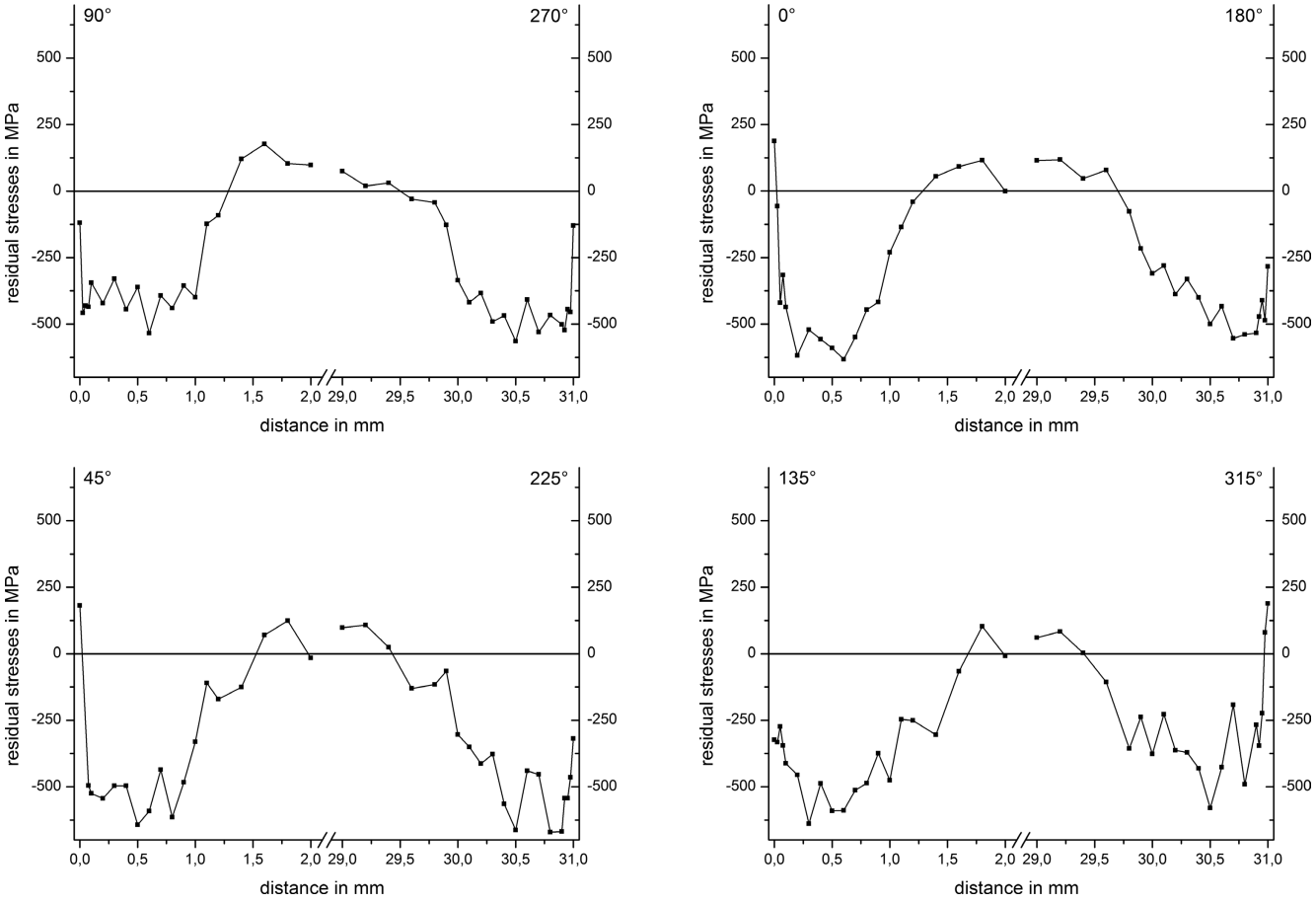

Fig. 10. Longitudinal residual stresses as a function of the measuring depth in different angles along the circumference of notch n3

Bild 10. Längseigenspannungen als Funktion der Messtiefe in verschiedenen Winkeln entlang des Umfangs von Kerbe n3

4 Depth profiles

Prior to this investigation, finite element simulations were done in order to identify the residual stress state of case hardened parts after straightening. The focus of these simulations was not on quantitative results, but on recognizing general effects on the residual stress state. For this purpose the simulation was carried out at first using homogeneous material. After that, hardened surface layers were added to simulate the effect of case hardening. Finally surface damage was included in the simulation by reducing the yield point directly on the surface. The bending deflection was set to a relatively high value, so that changes in the residual stress state could be clearly indentified. Not included in the model are transformations of retained austenite and initial residual stresses due to heat treatment. The resulting standardized longitudinal residual stresses as a function of the standardized bending height are shown in Figure 9. The bending height starts at the compression loaded side since the straightening stamp strikes there and ends on the tension loaded side. The left diagram corresponds to the homogeneous material. Due to plastic deformations that increase from core to surface, residual stresses were formed on the surface, which are compensated by alternating maxima in the core region. The result is a classical residual stress state with three zero crossings that shows tensile residual stresses at the previously compression loaded side and compressive residual stresses at the previously tension loaded side. The diagram in the middle shows the results of the case hardened material. The core region reacts as it is described for homogeneous material, but according to the high strength surface, the maximum of plastic deformation is shifted below the surface. As a result, new maxima have formed on the surface. In the right diagram the results of the case hardened material including surface damage can be seen. Compared to the previous residual stress state, new maxima were generated directly on the surface according to plastic deformation in the damaged surface layer with low yield strength. Because of the high number of measurements, the investigation of gradients in depth direction was limited to one single measurement location. Considering the axial location of the strongest straightening effect and the area of the most significant change in the residual stress state from the previous chapter, notch n3 was chosen. Measurements were taken in 45° steps along the circumference and displayed in combination with the opposite measuring point as it is shown in Figure 10. The neutral plane, that isn't affected by the straightening operation, is represented by the 90° to 270° plane. The residual stress values in this plane are distributed as it is expected for carbonitrided parts. Compressive residual stress maxima of about −500 MPa below the

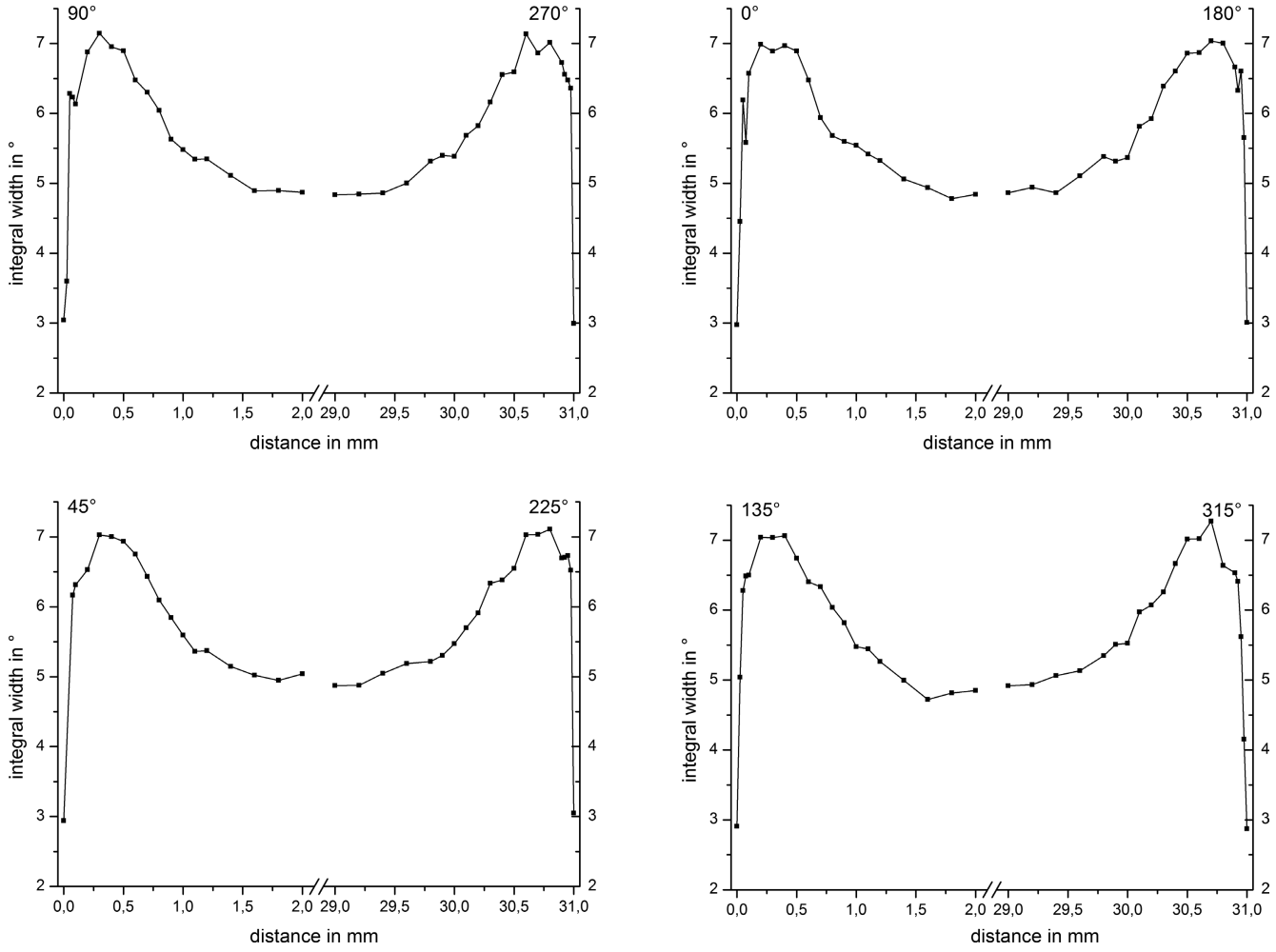

Fig. 11. Integral width values as a function of the measuring depth in different angles along the circumference of notch n3

Bild 11. Integralbreiten als Funktion der Messtiefe in verschiedenen Winkeln entlang des Umfangs von Kerbe n3

surface and low tensile residual stresses closer to the core region are observed. Along the bending height (0° to 180° plane) this initial state remains unchanged except of the compression loaded side (0°). Like it is described in the previous chapter, tensile residual stresses were formed due to plastic deformation during the straightening operation. This effect is limited to the surface layer and reaches up to 50 µm. Although the highest bending stresses are always located on the surface, this shallow depth indicates that the plastic deformation only took place in the area of the surface damage. This effect can also be seen at the 45° and 315° position. In total, the straightening operation doesn't affect the whole stress state of the shaft, but only the surface on the compression loaded side. The distribution of the integral width values follows the carbon content that was set during the carbonitriding process including the surface damage (see Figure 11). The curves for each of the eight different angles look very similar and it is not possible to recognize any alteration due to the straightening effects. The amount of retained austenite was measured to a depth of 0.4 mm. The curves in Figure 12 show maxima below the surface as it is expected for carbonitrided parts. Directly on the surface the amount of retained austenite was 0 %, which is remarkable since this effect can also be seen at every of the five notches that were included in the investigation. This doesn't seem to be caused during the carburizing process, because the values below the surface are normally distributed. Since the straightening operation only affects the surface, retained austenite cannot transform because there isn't any.

5 Conclusion

The effects of straightening operations on a hollow drive shaft which is used in an automobile gearbox were investigated with regard to its residual stress state and its microstructure. Therefore residual stress and integral width values were measured on the surface before and after the straightening operation. The measured circumferences were located on the cylindrical sections and in every notch of the straightening area. After the straightening process, measurements of residual stress-, integral width- and retained austenite gradients in depth direction were possible and done on the most affected notch. Comparing the residual stresses on the cylindrical sections before and after straightening, it is obvious, that these areas aren't participated on the straightening process. On the contrary, the residual stress states along the circumference of the notches changed significantly but only on the compression loaded side, since initial compressive residual stresses superimposed with compressive load stresses. As a result, tensile stresses appear in every notch that was considered. Based on

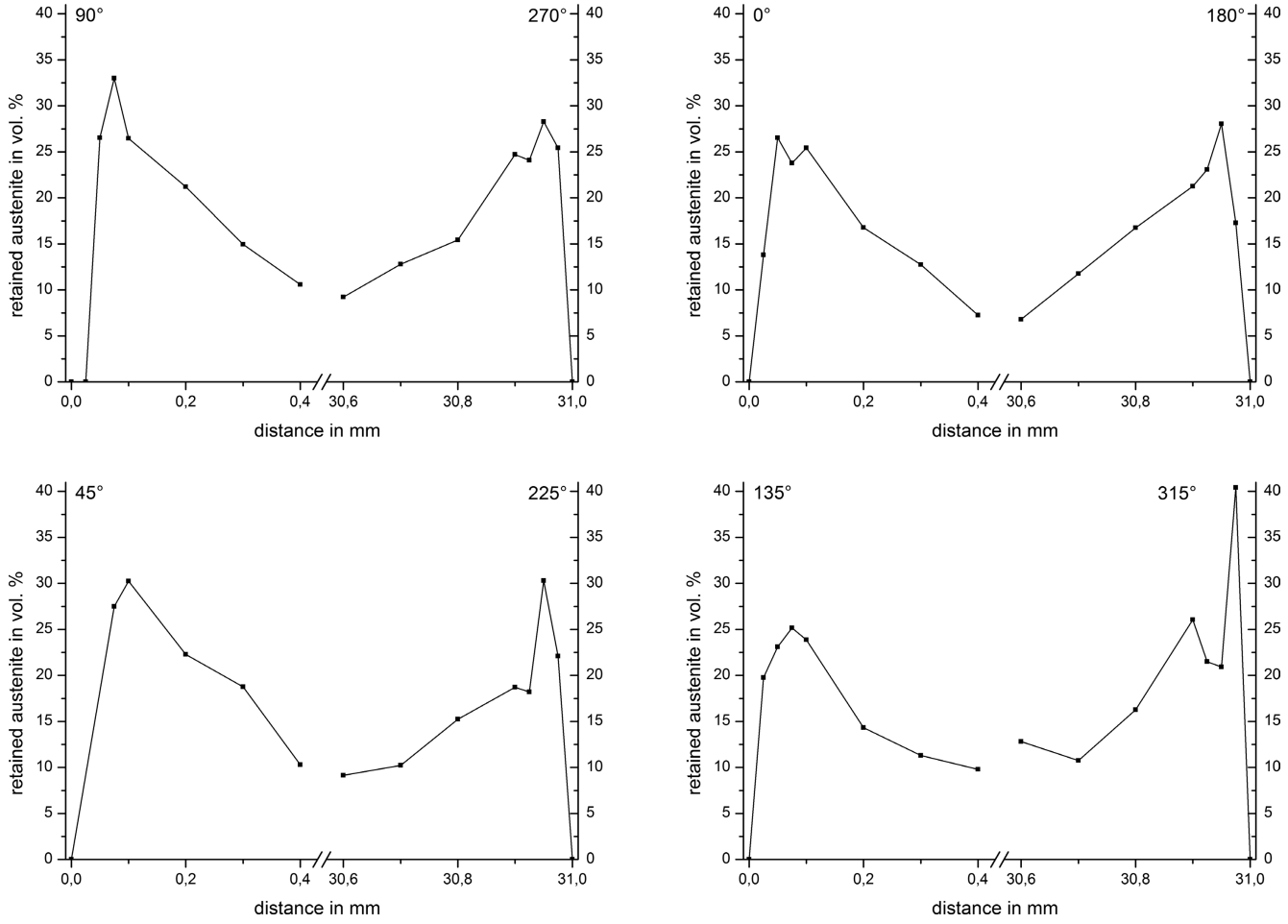

Fig. 12. The amount of retained austenite as a function of the measuring depth in different angles along the circumference of notch n3

Bild 12. Restaustenitgehalte als Funktion der Messtiefe in verschiedenen Winkeln entlang des Umfangs von Kerbe n3

these residual stress distributions, one representative notch was chosen to be investigated below the surface. It could be shown, that the initial residual stress state wasn't changed by the straightening operation except of a thin layer of about 50 µm below the surface on the compression loaded area between ±45° regarding the stamp direction. The plastic deformation, which is responsible for the changes in the residual stress values couldn't be traced in the integral width values as they are similar in every position along the circumference. The amount of retained austenite is distributed as expected for carbonitrided parts and doesn't transform to martensite under the bending stress but it is remarkable, that there isn't any retained austenite on the surface of every notch.

Acknowledgement

The presented results were obtained from research projects funded by the German Research Foundation DFG which is gratefully acknowledged. The authors would like to thank also for kind support of W. Schweinebraten VW AG Baunatal and M. Quandt (measurements).

Danksagung

Die in dieser Arbeit vorgestellten Ergebnisse wurden im Rahmen von Projekten gewonnen, die von der Deutschen Forschungsgemeinschaft DFG durch Sach- und Personalmittel unterstützt wurden. Dafür wird verbindlich gedankt. Ebenso wird Herrn W. Schweinebraten, VW AG Baunatal, für die Unterstützung und Herrn M. Quandt für die Durchführung der Messungen gedankt.

References

1. *Grosch, J.:* Fatigue resistance of carburized and nitrided steels. In: Thermochemical Surface Engineering of Steels, *Mittemeijer, E. J. M.; Somers, M. A.* (Eds.), Woodhead Publ., Cambridge, UK, 2014, pp. 209–240. – ISBN 978-0-85709-592-3
2. *Lübben, Th.; Zoch, H.-W.:* Einführung in die Grundlagen des Distortion Engineering. HTM J. Heat Treatm. Mat. *67* (2012) 5, pp. 275–290, DOI:10.3139/105.110161
3. *Zoch, H.-W.; Lübben, Th. (Eds.):* Proceedings 5th Int. Conf. on Distortion Engineering, 23-25.09.15, Bremen, Germany, 2015. – ISBN 978-3-88722-749-4
4. *Heeß, K; et al.:* Maß- und Formänderungen infolge Wärmebehandlung von Stählen: Grundlagen – Ursachen – Praxisbeispiele. 2nd ed., expert, Renningen, Germany, 2013
5. *Paul, M.; Vogel, W.:* Richten einsatzgehärteter Bauteile. HTM Haerterei-Techn. Mitt. *45* (1990) 2, pp. 90–97
6. *Scholtes, B.; Ellermann, A.; Baunack, D.; Kraus, A.; Zinn, W.:* Werkstofftechnische Grundlagen des Biegerichtens. HTM J. Heat Treatm. Mat. *70* (2015) 1, pp. 4–18, DOI:10.3139/105.110246
7. *Schott, C.; Ellermann, A.; Zinn, W.; Scholtes, B:* Consequences of Bend Straightening Processes on Residual Stresses and Strength of Quenched and Tempered Steels. HTM J. Heat Treatm. Mat. *71* (2016) 2, pp. 75–82, DOI:10.3139/105.110283
8. *Bartels, R. J.:* Einfluss des Restaustenits auf das Verformungsverhalten gehärteter Stähle. VDI Fortschritts-Berichte, Reihe 5, No. 162, VDI, Duesseldorf, Germany, 1989
9. *Tomala, V.; Hirsch, T.; Hoffmann, F.; Mayr, P.:* Versagensverhalten durchgreifend wärmebehandelter und gerichteter bauteilähnlicher Proben. HTM Haerterei-Techn. Mitt. *54* (1999) 6, pp. 392–399
10. *Randelius, M.; Aslund, J.; Hosseini, S.:* Straightening of case hardened bars before and after tempering. VBCentrum, VBC-R-2008-001, Swerea KIMAB, Stockholm, Sweden, 2008
11. *Haglund, S.; Kristoffersen, H.:* Simulation of Residual Stresses after Straightening of Induction Hardened Components. HTM J. Heat Treatm. Mat. *69* (2014) 3, pp. 165–172, DOI:10.3139/105.110223
12. *Fahlkrans, J.; Melander, A.; Gardstam, J.; Haglund, S.:* Straightening of induction hardened shafts – influence on fatigue strength and residual stress. HTM J. Heat Treatm. Mat. *67* (2012) 3, pp. 179–187, DOI:10.3139/105.110149
13. *Aslund, J.; Hosseini, S.; Haglund, S.:* Influence of straightening on fatigue properties – a study of bending fatigue and residual stresses of case hardened SS2511 steel. VBCentrum, VBC-R-2009-004, Swerea KIMAB, Stockholm, Sweden, 2009
14. *Clausen, B.; Hoffmann, F.; Zoch, H.-W.:* Beeinflussung der Randschicht durch die Einsatzhärtung. HTM J. Heat Treatm. Mat. *63* (2008) 6, pp. 326–336, DOI:10.3139/105.100473
15. *Macherauch, E.; Müller, P. Z.:* Das $\sin^2\psi$-Verfahren der röntgenographischen Spannungsmessung. Z. Angew. Physik 13 (1961), pp. 305-312

Bibliography

DOI:10.3139/105.110320
HTM J. Heat Treatm. Mat.
72 (2017) 3; page 145-153

ISSN 1867-2493